

Deconvolution and the Magnetic Pair Distribution Function

Kane Fanning

A senior thesis submitted to the faculty of  
Brigham Young University  
in partial fulfillment of the requirements for the degree of  
Bachelor of Science

Benjamin Frandsen, Advisor

Department of Physics and Astronomy

Brigham Young University

April 2022

Copyright © 2022 Kane Fanning

All Rights Reserved

## ABSTRACT

### Deconvolution and the Magnetic Pair Distribution Function

Kane Fanning

Department of Physics and Astronomy, BYU

Bachelor of Science

The potential utility of using the mathematical operation of deconvolution to improve the resolution of the magnetic pair distribution function produced from neutron scattering data is investigated. A standard deconvolution algorithm found in the Python library SciPy shows encouraging results, but introduces artifacts that are difficult to remove. Modeling the convolution inherent in the magnetic pair distribution function as matrix multiplication and then using the Moore-Penrose pseudoinverse to simulate deconvolution is also explored. We conclude that deconvolution holds significant promise as a method for increasing the resolution of experimentally determined magnetic pair distribution functions.

Keywords: magnetic pair distribution function, pair distribution function, convolution, deconvolution

## ACKNOWLEDGMENTS

I am grateful to many people: David Fanning, for the effect he has had on my mind; Benjamin Frandsen, for the effect he has had on my education; and Erika Shore, for the effect she has had on my happiness.



# Contents

<b>Table of Contents</b>	<b>v</b>
<b>List of Figures</b>	<b>vii</b>
<b>1 Introduction</b>	<b>1</b>
1.1 Atomic and Magnetic Structure . . . . .	1
1.2 Atomic and Magnetic Pair Distribution Function . . . . .	2
1.3 Convolution and Deconvolution . . . . .	4
1.4 Deconvolution and the Magnetic Pair Distribution Function . . . . .	6
<b>2 Methods</b>	<b>9</b>
2.1 Use of Simulated Data . . . . .	9
2.2 Determining Success or Failure of Algorithms . . . . .	10
2.3 Solution Methods Investigated . . . . .	11
<b>3 Results</b>	<b>13</b>
3.1 SciPy . . . . .	13
3.2 Approximating Convolution with Matrix Multiplication . . . . .	15
<b>4 Conclusions</b>	<b>17</b>
<b>Bibliography</b>	<b>19</b>
<b>Index</b>	<b>21</b>



# List of Figures

1.1	PDF conceptual example . . . . .	3
1.2	Convolution example . . . . .	5
1.3	True mPDF vs measured mPDF . . . . .	6
3.1	Artifacts introduced by deconvolution . . . . .	14
3.2	Deconvoluted mPDF after smoothing . . . . .	15
3.3	Matrix approximation of measured mPDF and true mPDF . . . . .	16





# Chapter 1

## Introduction

### 1.1 Atomic and Magnetic Structure

Understanding the properties of a given material depends critically on understanding the atomic structure of that material and, in many cases, its magnetic structure. Atomic structure refers to the physical location of atoms relative to each other in a material. Magnetic structure refers to the relative location, strength, and orientation of magnetic moments in a material. Determining these structures for an unknown or new material is an important step in the development of technologically relevant materials, and thus developing methods that can more quickly and accurately determine the atomic or magnetic structure of a material is a valuable pursuit.

Several crystallographic methods exist for determining the arrangement of atoms in a material. X-ray diffraction, for example, involves directing a beam of X-rays at a material, measuring how they diffract, and then comparing the measured diffraction pattern with diffraction patterns calculated from known, candidate crystal structures. One can then iteratively adjust the candidate crystal structure until one is found that produces a diffraction pattern similar to the measured one. Standard X-ray diffraction, then, produces a diffraction pattern for a material—the distribution of

scattered photons as a function of angle. If the material has a well-ordered crystal structure, the scattered intensity is very strong at certain angles, resulting in sharp peaks in the diffraction pattern called Bragg peaks. These peaks correspond to angles that satisfy Bragg's law and result in coherent scattering from the material. This provides information about the average crystalline structure of a material, like how far apart two adjacent layers in the crystal are. Because small breaks in the average structure of a material do not cause coherent scattering, they do not produce Bragg peaks and are very difficult to detect in the diffraction patterns produced by traditional X-ray diffraction. A similar effect is observed in the different diffraction patterns produced by light impinging on two narrow slits versus many narrow slits. As the number of slits increases from two, the intensity of the principle maximum increases and its width decreases relative to the principle maximum produced in the two slit diffraction pattern, similar to a Bragg peak becoming very sharp as millions of uniform crystal layers all diffract the impinging X-rays in the same manner. Thus while X-ray diffraction is extremely useful for many applications, additional methods are needed to more accurately characterize the short-range breaks in the average structure of a material. More information about X-ray diffraction can be found in the textbooks (Massa 2004) and (Clegg 2015).

## 1.2 Atomic and Magnetic Pair Distribution Function

The pair distribution function (PDF) provides information about the arrangement of atoms over short distances, and is very effective for studying local breaks in the average structure of a material. More specifically, the pair distribution function maps linear distances to a value proportional to the likelihood of finding two atoms separated by that distance. For example, in Figure 1.1, the PDF has spikes in the blue and red regions, as the likelihood of finding an atom a distance  $r$  away from the center green atom is very high when  $r$  is in the red and blue regions.

While closely related to X-ray diffraction, PDF analysis makes use of both Bragg scattering

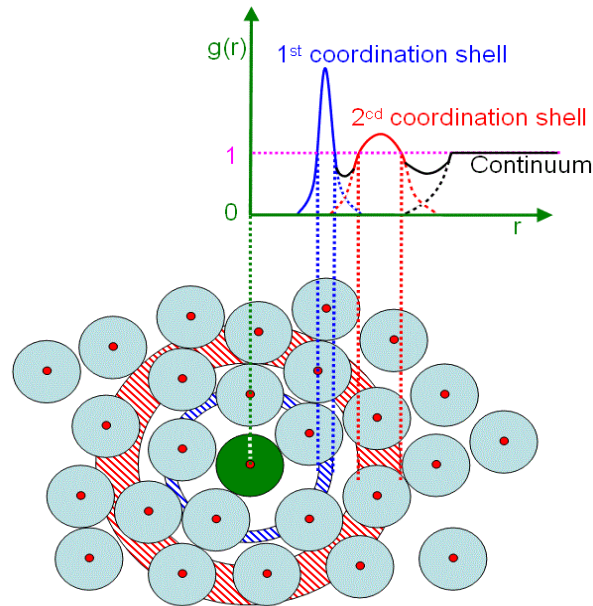


**Figure 1.1** A simplified depiction of a material and its pair distribution function. The horizontal axis is distance, often measured in angstroms, and the vertical axis is a dimensionless quantity proportional to the likelihood of finding a pair of atoms separated by a distance  $r$ . The green atom in the center is taken to be the origin, with distances measured radially outwards. For this material, as we move away from the green atom, we are very likely to find another atom in the blue or red region, and thus the pair distribution function has spikes in those regions of  $r$ . Source: <https://www.globalsino.com/EM/image2/3097.GIF>

from the average crystallographic structure and diffuse scattering from local deviations from the average structure, and as a result provides more information about the short-range structure of a material. More information about pair distribution function analysis can be found in the article (Petkov 2012) and its references, and in the textbook (Egami 2003).

The magnetic pair distribution function (mPDF) is similar to the atomic pair distribution function, but provides information about how likely two magnetic moments are to be separated by a given distance and what their relative orientation is. Because the magnetic moments in a material are produced by the atoms, there is a large degree of correlation between a material's atomic and magnetic PDFs. The magnetic pair distribution function, however, provides orientational information that is not present in the atomic PDF—a positive spike in the mPDF at distance  $r$  indicates a

high likelihood of finding two magnetic moments separated by a distance  $r$  aligned ferromagnetically (i.e. parallel), while a negative peak at  $r$  indicates a high likelihood of finding two magnetic moments separated by a distance  $r$  aligned antiferromagnetically (i.e. antiparallel).

Both the PDF and mPDF are produced by taking the Fourier transform of data gathered in scattering experiments. The PDF can be produced from data gathered in X-ray or neutron scattering experiments, while the mPDF can be produced exclusively from data gathered in neutron scattering experiments. The neutron's neutral electric charge but nonzero magnetic moment makes it an effective probe for determining the magnetic structure of a material.

### 1.3 Convolution and Deconvolution

Convolution is a mathematical operation that, in informal terms, describes how the shape of one function is modified by the shape of another. In the continuous case, the convolution of two functions  $f$  and  $g$  is given by

$$(f * g)(t) = \int_{-\infty}^{\infty} f(\tau)g(t - \tau)d\tau, \quad (1.1)$$

while in the discrete case, the convolution of two vectors  $\mathbf{f}$  and  $\mathbf{g}$  is given by

$$(\mathbf{f} * \mathbf{g})[n] = \sum_{m=-\infty}^{\infty} \mathbf{f}[m]\mathbf{g}[n - m]. \quad (1.2)$$

One might think of convolution as a "blending" of two functions (Weisstein 2022a), or an operation that describes how the shape of one function affects the shape of another. If one of these functions is Gaussian or Gaussian-like, the original signal is often "broadened" and "smoothed," as illustrated in Figure 1.2. Deconvolution is the inverse operation of convolution. Convolution and deconvolution are commonly used in many areas, including signal processing, where the output of an instrument is often described as the convolution of the true signal and the instrument's impulse response, and image processing, where the image captured by a sensor is the convolution between

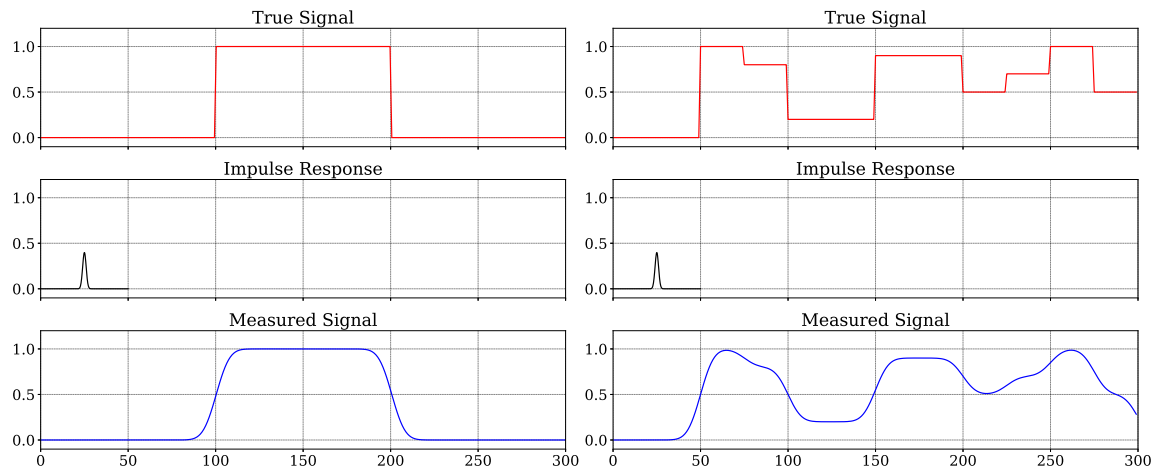


**Figure 1.2** An example of the convolution of two functions. On the left, the signal is a simple square pulse; on the right is a more complicated sum of step functions. In both cases the impulse response (or the function the signal is convolved with) is a Gaussian impulse with variance 1.

the point sources of light and the sensor's point-spread function. In these and other applications, deconvolution is used to try to recover the true signal from the measured signal. While technically an "ill-posed problem (Weisstein 2022b)," in many cases deconvolution is a simple and reliable tool. For example, when the measured signal and the convolving function (i.e. impulse response function, point-spread function, etc.) are both precisely known and with a high enough signal to noise ratio, the true signal is obtained by deconvolving the measured signal with the convolving function. In practice, however, the deconvolution of two functions is usually calculated using several Fourier and inverse Fourier transforms, which can fail to produce meaningful results if the measured signal's signal-to-noise ratio is too low, or if other requirements for stability are not met. It is for this reason that, while simple in theory, obtaining the original signal from the convoluted signal and the convolving function is often difficult or impossible.

## 1.4 Deconvolution and the Magnetic Pair Distribution Function

The resolution of the mPDF pattern obtained from a given magnetic material is limited by that material's magnetic form factor. The magnetic form factor for a given material describes how the magnetic scattering is suppressed at large scattering angles, and is a result of the finite spatial extent of the wave functions of the unpaired electrons that are doing the scattering. More detailed information about the theory of magnetic form factors can be found in (Zaliznyak & Lee 2005). For our purposes, it is enough to know that the magnetic form factor causes the magnetic scattering intensity to get exponentially smaller as the scattering angle increases and introduces a "broadening" or "smoothing out" effect to the mPDF. An example of this broadening effect is given by the blue curve in Figure 1.3.

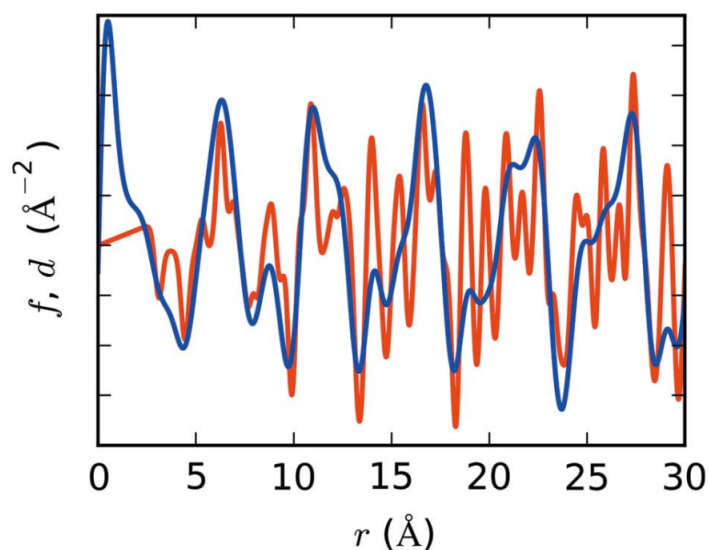


**Figure 1.3** An example of what a "true" mPDF (red) and "measured" mPDF (blue) might look like, in this case calculated for MnO. The goal of this research is to produce the red curve from the blue curve by twice deconvolving the blue curve with the Fourier transform of the magnetic form factor. Source: <https://doi.org/10.1107/S205327331500306X>

More explicitly, if  $I(Q)$  is the scattering intensity measured by the detectors in an experiment, then

$$S(Q) = \frac{I(Q)}{f(Q)^2}, \quad (1.3)$$

where  $S(Q)$  is the magnetic structure factor,  $f(Q)$  is the magnetic form factor of the given material, and  $Q$  is the domain coordinate in reciprocal space, which is related to the scattering angle. The magnetic structure factor is important in that the true magnetic pair distribution function for a material is given by the Fourier transform of it,  $\mathcal{F}\{S(Q)\}$ .

To calculate  $\mathcal{F}\{S(Q)\}$ , one might simply divide the observed intensity  $I(Q)$  by the square of a material's approximate magnetic form factor and take the Fourier transform, as suggested by equation (1.3). However, because the magnetic form factor is typically very small beyond approximately  $5 \text{ \AA}^{-1}$ , dividing by the square of it can introduce distortions and amplify noise (Frandsen & Billinge 2016). To avoid this, we can first compute the Fourier transform of  $S(Q)$  multiplied by the form factor squared,

$$\mathcal{F}\{S(Q) \cdot f(Q)^2\} = \mathcal{F}\{I(Q)\}. \quad (1.4)$$

Recalling that the convolution theorem states that pointwise multiplication in Fourier space is equivalent to convolution in real space, we can rewrite equation (1.4) as

$$\mathcal{F}\{S(Q)\} * \mathcal{F}\{f(Q)\} * \mathcal{F}\{f(Q)\} = \mathcal{F}\{I(Q)\}, \quad (1.5)$$

where  $*$  represents the mathematical operation of convolution. If we can then twice *deconvolve* both sides of equation (1.5) with  $\mathcal{F}\{f(Q)\}$ , or equivalently deconvolve once with the new quantity  $[\mathcal{F}\{f(Q)\} * \mathcal{F}\{f(Q)\}]$ , we will have then obtained the desired quantity  $\mathcal{F}\{S(Q)\}$  without ever dividing by the square of the magnetic form factor.

The goal of this research, then, is to explore deconvolution as an alternative method of approximating the true mPDF (red curve in Figure 1.3) from the measured mPDF collected in a neutron

scattering experiment (blue curve in Figure 1.3), with the hope of producing a new, reliable, and rapid method that does not involve dividing by the square of the magnetic form factor.



# Chapter 2

## Methods

### 2.1 Use of Simulated Data

In order to more rapidly determine the potential utility of deconvolution, all investigation was performed using a single simulated data set—data that was calculated analytically using a computer, rather than experimentally collected. Because deconvolution is especially sensitive to a signal's signal-to-noise ratio, using experimentally collected data could lead to errors and difficulties that obscure the effectiveness of the deconvolution algorithm being tested. To avoid this and other potential issues, the data used in this investigation was created from calculations of the magnetic pair distribution function for a known material, MnO. In other words, we explicitly calculated what the mPDF would be for MnO using its known lattice structure and other parameters. In this sense, our simulated data provides an exact target to compare against—the "true" mPDF. The red curve in Figure 1.3 is the true mPDF for MnO. The approximate magnetic form factor of MnO is also known, and can thus be convolved twice with the true mPDF to produce an mPDF similar to what an actual neutron scattering experiment on MnO would yield. This double convolution of the true mPDF with the approximate magnetic form factor can be referred to as the "measured"

mPDF, and for MnO, is given by the blue curve in Figure 1.3. The benefit of using simulated data is that this measured mPDF has no noise, which would certainly be present in experimental data. Thus our simulated data provides both a true mPDF to compare our results against, and a noiseless curve simulating the type of data that would be gathered in a real-world experiment, which we can attempt to deconvolve. If the various deconvolution algorithms employed succeed in producing a curve close to the true mPDF, then deconvolution may be a viable method for approximating the true mPDF from experimental data.

When testing some deconvolution algorithms, the magnetic form factor of the material was often assumed to be Gaussian. Most materials have a magnetic form factor that is well approximated by a sum of Gaussians, so this approximation is reasonable and adequate for our purposes.

## 2.2 Determining Success or Failure of Algorithms

Our experimental method consisted primarily of developing and running various deconvolution algorithms on the measured mPDF and visually comparing the results to the true mPDF. Algorithms would then be tweaked until the deconvolved mPDF most resembled the true mPDF. Smoothing functions or peak-sharpening algorithms were also used post-deconvolution to get the deconvolved mPDF closer to the true mPDF.

Visual similarity was judged primarily based on the alignment of peaks between the deconvolved and true mPDF. While more exact error metrics will certainly be needed in the future, in this preliminary stage, visual comparison is more than adequate for determining the feasibility of a method, and whether or not it merits further pursuit.

## 2.3 Solution Methods Investigated

Several standard deconvolution algorithms were used and investigated. Matlab's `deconv` function and SciPy's `scipy.signal.deconvolve` method are effectively the same algorithm and were the first algorithms explored. Both make use of long division to find the deconvolution of two vectors and are commonly used in many signal-processing applications.

In addition to standard deconvolution algorithms, a matrix multiplication method was also explored. One-dimensional convolution can be modeled as a linear matrix equation of the form

$$\mathbf{Ax} = \mathbf{b}, \quad (2.1)$$

where  $\mathbf{x}$  is the true mPDF (a vector of length  $n$ ),  $\mathbf{b}$  is the broadened experimentally measured mPDF (a vector of length  $n$ ), and  $\mathbf{A}$  is an  $n \times n$  matrix that simulates the effect of convolving the true mPDF with the Fourier transform of the magnetic form factor twice. Written in this form, the task of discovering the true mPDF  $\mathbf{x}$  consists of solving a linear matrix equation, for which many methods exist, rather than performing numeric deconvolution. That is, given the form of equation (2.1), computing the true mPDF consists of calculating  $\mathbf{A}^{-1}$  such that

$$\mathbf{x} = \mathbf{A}^{-1}\mathbf{b}.$$

The first task is to construct a matrix  $A$  that accurately replicates the "smoothing out" effect that the magnetic form factor has on the true mPDF. One possibility is a row-stochastic matrix with a Toeplitz interior, a simple example of which might look like

$$\begin{bmatrix} 1 & 0 & 0 & 0 & 0 & 0 \\ 0.2 & 0.6 & 0.2 & 0 & 0 & 0 \\ 0 & 0.2 & 0.6 & 0.2 & 0 & 0 \\ 0 & 0 & 0.2 & 0.6 & 0.2 & 0 \\ 0 & 0 & 0 & 0.2 & 0.6 & 0.2 \\ 0 & 0 & 0 & 0 & 0 & 1 \end{bmatrix}. \quad (2.2)$$

In this case, the endpoints of whatever signal is multiplied by this matrix are fixed, while each interior point  $p_i$  is given by  $p_i = 0.2(p_{i-1}) + 0.6(p_i) + 0.2(p_{i+1})$ . To accurately model the smoothing effect the magnetic form factor has on the mPDF, a more complicated matrix is needed, as well as a way to reliably produce this matrix for an arbitrary material based only on *a priori* knowledge of its chemical composition. One way to do this is to use an approximation of the magnetic form factor to construct the rows of the matrix  $A$ , such as

$$\langle j_o(s) \rangle = Ae^{-as^2} + Be^{-bs^2} + Ce^{-cs^2} + D, \quad (2.3)$$

with coefficients experimentally determined and accessible at (Brown 1997).

Construction of  $\mathbf{A}$  using the Fourier transform of the squared magnetic form factor is necessary to apply this method to experimental data, but because our simulated data includes the true mPDF  $\mathbf{x}$ , the concept can be tested on an  $\mathbf{A}$  matrix constructed using a single Gaussian, rather than the sum in equation (2.3).

# Chapter 3

## Results

### 3.1 SciPy

Attempting to deconvolve our simulated data with the Fourier transform of an (approximate) squared magnetic form factor using SciPy's `scipy.signal.deconvolve` produced results close to the true mPDF, but with unusual artifacts. One common artifact can be seen in Figure 3.1, in which deconvolution of the measured mPDF with the magnetic form factor produced periodic, extremely high-amplitude spikes. In between the spikes, the agreement between the true mPDF and the approximation of it produced by `scipy.signal.deconvolve` is high.

Because the spikes are so periodic, they should be easily detectable, and a rudimentary smoothing algorithm was developed to remove them. In brief, this algorithm progressively takes a fixed-length subsample from the deconvoluted curve and calculates the standard deviation of that subsample. In regions where the standard deviation is above a certain threshold value (e.g. due to a large spike in the deconvoluted signal), the subsample is replaced with an interpolation extending from a few points before the beginning of the subsample to a few points after the end of the subsample. The algorithm can iterate several times with different standard deviation thresh-

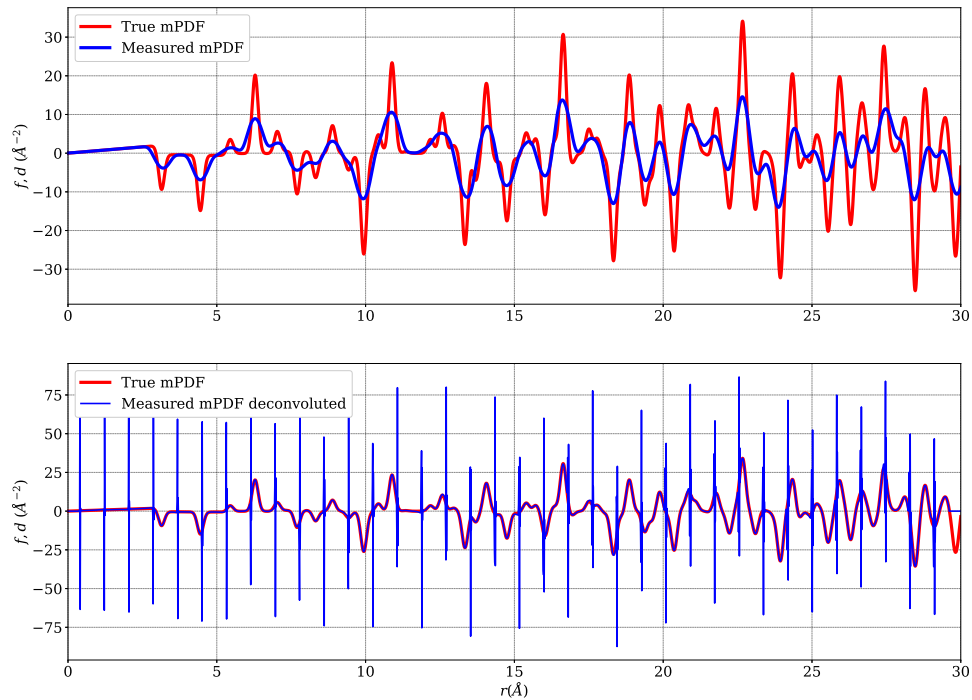


**Figure 3.1** An example of one type of artifact seen while using `scipy.signal.deconvolve`. The upper panel features the true mPDF for MnO in red and the measured mPDF in blue, both computed using simulated data. The lower panel features the same true mPDF in red, but in blue is now the measured mPDF twice deconvolved with the Fourier transform of the magnetic form factor. In between the large, periodic spikes, the agreement between the true mPDF and the deconvolved approximation of it is quite high.

olds depending on the iteration. The subsample length can also be tuned, and the type of interpolation can be adjusted (linear, quadratic, cubic, etc.). The interpolation is performed using `scipy.interpolate.interp1d`.

The approximation of the true mPDF produced by `scipy.signal.deconvolve` and smoothed using the described algorithm is compared to the true mPDF in Figure 3.2. Nearly all the spikes are removed, with only a few low-amplitude spikes remaining for low  $r$  values. The agreement over the rest of the domain is significant but imperfect, with a few sharp jumps and other artifacts

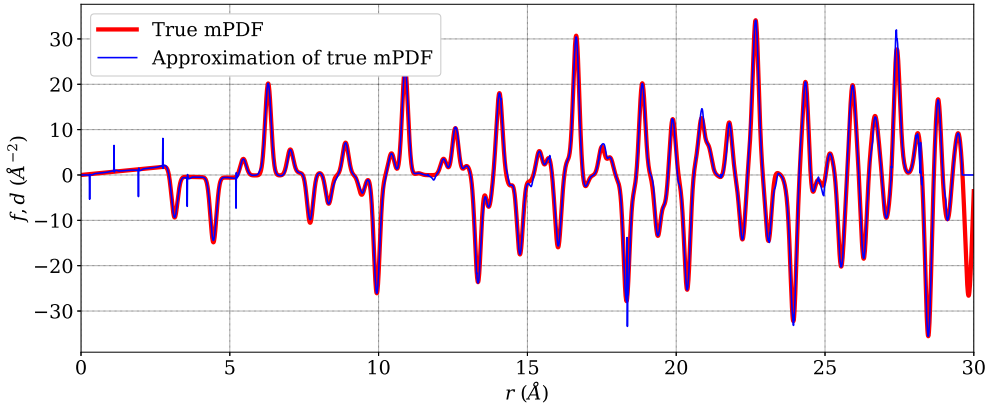


**Figure 3.2** A comparison of the true mPDF to the smoothed, deconvoluted approximation to it.

remaining. Despite the remaining spikes, fewer discontinuities and sharp artifacts seem present in lower  $r$  values than higher  $r$  values. It is likely that both the small spikes at low  $r$  values and the too-sharp peaks at larger  $r$  values could be removed with a more robust smoothing algorithm.

## 3.2 Approximating Convolution with Matrix Multiplication

Modeling convolution as a linear matrix equation and solving for the true mPDF using the Moore-Penrose pseudoinverse yielded promising results. The left panel of Figure 3.3 contains the true mPDF  $\mathbf{x}$ , the measured mPDF  $\mathbf{b}$ , and the approximation of the measured mPDF  $\mathbf{Ax}$ , where the rows of  $\mathbf{A}$  are created using a Gaussian with standard deviation tuned to best approximate the measured mPDF. (With experimental data, the matrix  $\mathbf{A}$  would have to be created using only knowledge of the magnetic form factor, as there is no true mPDF available to multiply by  $\mathbf{A}$  and judge the accuracy.) The agreement between the blue and gold curves in the left panel confirms that the measured mPDF can be very accurately approximated with matrix multiplication.

The right panel of Figure 3.3 includes the true mPDF, the measured mPDF, and the approximation of the true mPDF  $\mathbf{A}^+\mathbf{b}$ , where  $\mathbf{A}^+$  is the Moore-Penrose pseudoinverse (Moore 1920; Penrose

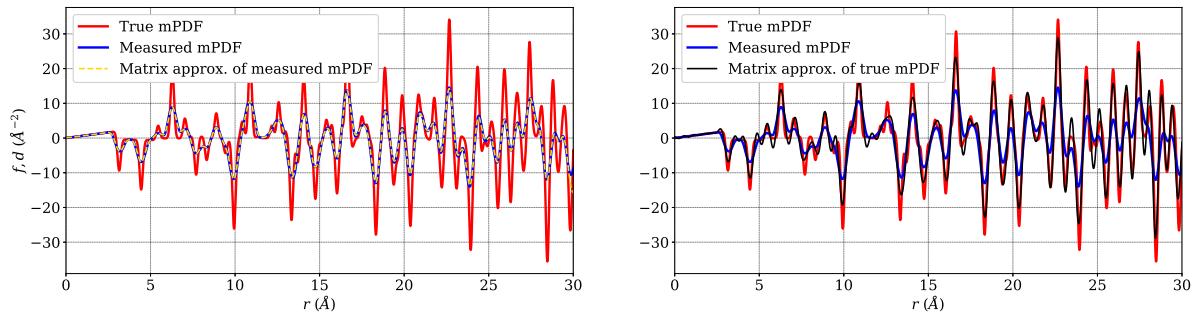


**Figure 3.3** The left panel contains the true mPDF  $\mathbf{x}$ , the measured mPDF  $\mathbf{b}$ , and the approximation of the measured mPDF  $\mathbf{A}\mathbf{x}$ , where  $\mathbf{A}$  is constructed using a Gaussian tuned to best match the measured mPDF. Despite not using the magnetic form factor to create the matrix  $\mathbf{A}$ , the agreement between the measured mPDF and its approximation is excellent. The right panel contains the true mPDF, the measured mPDF, and the approximation of the mPDF  $\mathbf{A}^+\mathbf{b}$ , where  $\mathbf{A}^+$  is the Moore-Penrose pseudoinverse of  $\mathbf{A}$  (constructed only with singular values greater than 0.1).

1955). This approximation of the true mPDF captures most all of the significant features of the true mPDF, and seems to do slightly better at larger values of  $r$ , in contrast to our results using `scipy.signal.deconvolve` and our smoothing algorithm (Figure 3.2). In Figure 3.3, the pseudoinverse was calculated using only singular values greater than one tenth of the largest singular value, with all other singular values set to zero.



# Chapter 4

## Conclusions

Deconvolution certainly holds promise as an alternative method for producing the magnetic pair distribution function from neutron scattering data. SciPy's standard deconvolution algorithm seems to work well, but introduces artifacts that are difficult to predict and require lengthy manual removal that is often very finicky. Developing an automated method that accepts neutron scattering data for an arbitrary material and reliably returns the mPDF using this deconvolution algorithms will require significant amounts of further work, but seems possible.

Casting the problem as a linear matrix equation is perhaps the avenue most worth further consideration, primarily because solving linear matrix equations is a well-researched problem, and a method that would work well to solve our problem likely already exists. Our preliminary results are encouraging, with the main challenge being producing a matrix that will accurately approximate the double convolution of the true mPDF with the Fourier transform of the magnetic form factor. In this exploration, we had the benefit of possessing the true mPDF to test the accuracy of our matrix on, but in a real experiment we will have to produce a similar matrix without being able to compare it. However, once the matrix is created, this method seems more reliable and produces far fewer inexplicable artifacts than `scipy.signal.deconvolve`. For this reason, this method could lend itself better to automation.

The greatest challenge yet to be faced is likely applying any of these methods to actual experimental data. All of the methods explored here become less robust in the presence of noise. Even working with noiseless data, artifacts have been introduced that are difficult to explain and remove; these difficulties are sure to increase with any decrease in the signal to noise ratio.

# Bibliography

- A. Oppenheim A. Willsky, S. N. 1996, Signals and Systems, 2nd edn., Prentice Hall Signal Processing Series (Upper Saddle River, NJ: Prentice Hall)
- Billinge, S. J. L. 2019, Philosophical Transactions of the Royal Society A: Mathematical, Physical and Engineering Sciences
- Brown, P. J. 1997, Magnetic Form Factors, <https://www.ill.eu/sites/ccsl/ffacts/ffactnode1.html>
- Clegg, W. 2015, X-ray crystallography (Oxford Univ. Press)
- Egami, S. J. L. B. . T. 2003, Underneath the Bragg Peaks: Structural Analysis of Complex Materials, 2nd edn. (Oxford, United Kingdom: Pergamon Press)
- Farrow, C. L., & Billinge, S. J. L. 2009, Acta Crystallographica Section A Foundations of Crystallography, 65, 232
- Frandsen, B., & Billinge, S. J. L. 2016, Neutron News, 27, 14
- Frandsen, B. A., & Billinge, S. J. L. 2015, Acta Crystallographica Section A, 71, 325
- Frandsen, B. A., Yang, X., & Billinge, S. J. L. 2014, Acta Crystallographica Section A, 70, 3
- Massa, W. 2004, Crystal structure determination (Springer)
- McCallum, B. 1990, Optics Communications, 75, 101

Moore, E. H. 1920, *Bulletin of the American Mathematical Society*, 26, 394

Penrose, R. 1955, *Mathematical Proceedings of the Cambridge Philosophical Society*, 51, 406413

Petkov, V. 2012, *Characterization of Materials*, 2nd edn. (John Wiley & Sons, Inc.), 1361–1372

Squires, G. L. 2012, *Introduction to the Theory of Thermal Neutron Scattering*, 3rd edn. (Cambridge University Press)

Stéphane, M. 2009, in *A Wavelet Tour of Signal Processing (Third Edition)* (Boston: Academic Press), 59–88

Weisstein, E. W. 2022a, Convolution, [Online]. Available from: <https://mathworld.wolfram.com/Convolution.html>

—. 2022b, Deconvolution, [Online]. Available from: <https://mathworld.wolfram.com/Deconvolution.html>

Wirestam, R., & Ståhlberg, F. 2005, *Magnetic Resonance Materials in Physics, Biology and Medicine*, 18, 113

Zaliznyak, I., & Lee, S.-H. 2005, *Magnetic Neutron Scattering*, 3–64

# Index

artifacts, 17  
atomic structure, 1, 2  
automation, 17  
  
Bragg peaks, 1  
broadened, 15  
  
coherent scattering, 1  
convolution, 2, 4, 15  
crystalline structure, 1  
crystallography, 1  
  
deconvolution, 4, 9, 15  
diffuse scattering, 1  
discrete, 4  
  
Fourier transform, 4  
  
Gaussian, 15  
  
impulse response, 4  
interpolation, 13  
  
linear matrix equation, 15, 17  
  
magnetic form factor, 2  
magnetic structure, 1, 2  
Matlab, 13  
measured mPDF, 9  
MnO, 1, 9  
Moore-Penrose pseudoinverse, 15  
mPDF, 2, 9  
  
PDF, 2  
point-spread function, 4  
pseudoinverse, 15  
  
resolution, 2  
  
SciPy, 9, 13, 15, 17  
signal processing, 4  
signal-to-noise ratio, 9  
simulated data, 9  
smoothing algorithm, 13  
spike, 13  
  
Toeplitz matrix, 15  
true mPDF, 9  
  
X-ray diffraction, 1